2008 IEEE International Conference on
Robotics and Automation
Pasadena, CA, USA, May 19-23, 2008

Detection and Real-time Correction of Faulty Visual Feedback in Atomic Force Microscopy Based Nanorobotic Manipulation

Lianqing Liu*†§, Ning Xi†, Yilun Luo†, Yuechao Wang*, Jiangbo Zhang†, Guangyong Li‡

***Abstract*—One of the main roadblocks to Atomic Force Microscope (AFM) based nanomanipulation is lack of real time visual feedback. Although the model based visual feedback can partly solve this problem, its unguaranteed reliability due to the inaccurate models in nano-environment still limits the efficiency of AFM based nanomanipulation. This paper introduce a Real-time Fault Detection and Correction (RFDC) method to improve the reliability of the visual feedback. By utilizing Kalman filter and local scan technologies, the RFDC method not only can real-time detect the fault display caused by the modeling error, but also can on-line correct it without interrupting manipulation. In this way, the visual feedback keeps consistent with the true environment changes during manipulation, which makes several operations being finished without a image scanning in between. The theoretical study and the implementation of the RFDC method are elaborated in this paper. Experiments of manipulating nano-particles have been carried out to demonstrate the effectiveness and efficiency of the proposed method.**

I. INTRODUCTION

Atomic force microscopy (AFM) [1] has been proven to be a powerful technique to study sample surfaces down to the nanometer scale. Not only can it characterize sample surfaces, it can also be used as a manipulation tool to change the sample surface taking advantage of its high resolution and alignment accuracy. Nanolithography [2],[3] and nanomanipulation [4]-[8] has been successfully performed and brought some new breakthroughs in different research areas. But the problem of lacking real time visual feedback still limits its efficiency and hinders its application as a nanomanipulation tool. When going manipulation with AFM, each step of the operation has to be verified by a new image scan that often takes several minutes. This scan-design-manipulation-scan cycle is time consuming and makes complex assembly task impossible to be carried out.

To enhance the efficiency of AFM based manipulation, some methods based on virtual reality have been developed [9], [10]. Although a virtual reality can display a static virtual environment and a dynamic tip position, it does not display the environment changes during manipulation. The operator is still 'blind' because the environment changes are not updated in real time. To solve this problem, an augmented reality system has been developed in [11]. With this method, not only a movie-like visual feedback is provided, a force feedback is also displayed through a haptic device. The operator can go on manipulation under the assistance of force feedback and visual feedback. But this kind of visual display is the calculated real-time changes of the real environment from the object's behavior model [12], not the true manipulation results. Due to the complications and uncertainties of the nano-world, such as surface tension, van der Waals force, capillary force and so on, it is difficult to accurately describe the object's behavior with a model. Thus the visual feedback may not represent the true environment changes. As a result, a nanomanipulation may fail due to the fault display. Active probe is used as an adaptable end effector to detect this situation [13], by actively control the rigidity of the cantilever, a high sensitive interaction force feedback can be obtained, through which the mismatch between the visual display and true environment changes can be sensed by the operator. However, a complete image scan is still needed to correct the display error. Thus it is imperative to find a method to generate a reliable visual feedback without image scan in between. In this paper, an Real-time Fault Detection and Correction (RFDC) method is proposed to approach this goal. The RFDC method is implemented by two key technologies: Kalman filter and local scan. During manipulation, the manipulation process is real-time monitored by the Kalman filter. Once the visual display loses match with the true environment, local scan is performed to obtain the true manipulation result and correct the fault display. Since only several lines are scanned, local scan can be finished in several tens of milliseconds without operator's perceiving. Therefore, fault display caused by the model errors can be compensated without AFM image scan in between. By combining RFDC method with our formerly developed augmented reality system, the reality of the visual display is greatly improved. The experimental results show that the mismatch between the visual display and the true environments during manipulation can be real-time detected and corrected without interrupting the manipulation. Therefore, the efficiency of AFM based nanomanipulation has been significantly improved.

The remainder of this paper first gives an overview of the system structure, then discusses how to detect the fault display and correct it, Finally, the implementation and experimental results are presented.

II. THE AUGMENTED REALITY SYSTEM WITH REAL-TIME FAULT DETECTION AND CORRECTION

The augmented reality system provides an operator with real-time movie-like visual display and force feedback during

*Shenyang Institute of Automation, Chinese Academy of Sciences, Shenyang, Liaoning Province, 110016, China.
†Department of Electrical and Computer Engineering, Michigan State University, East Lansing, MI 48823, USA.
‡Department of Electrical and Computer Engineering, University of Pittsburgh, Pittsburgh, PA 15621, USA.
§Graduate School of Chinese Academy of Sciences, Beijing, 100001 China.

E-amil address: xin@egr.msu.edu, lqliu@sia.cn

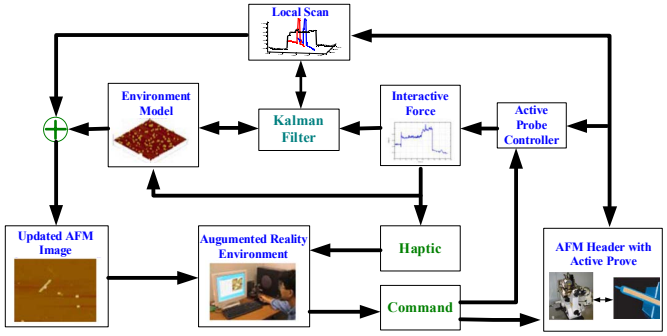

Fig. 1. The architecture of the augmented reality system enhanced by real-time fault detection and correction.

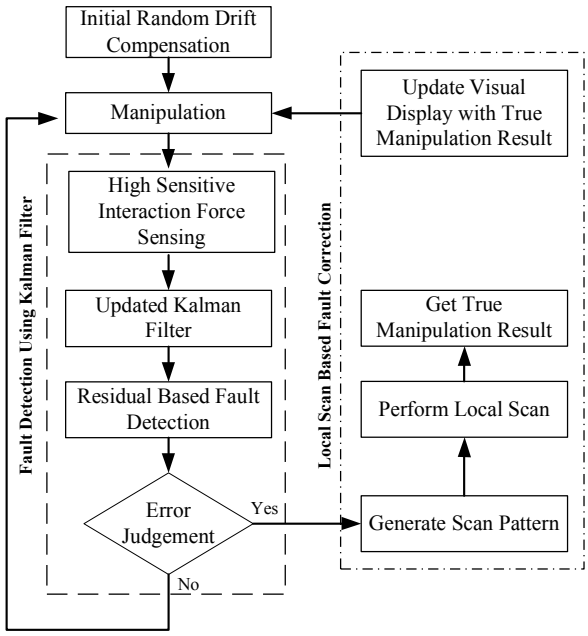

Fig. 2. The flowchart for the real-time fault detection and correction.

nanomanipulation. Since this visual display is achieved from the behavior models, it may not consistent with the true environment due to the models' inaccuracy. To improve the reliability of the visual display, an RFDC enhanced system architecture is developed as shown in Fig. 1. It mainly includes three subsystems, the AFM system, the augmented reality interface and the real-time control module. The bottom right is the AFM system, it is the execution unit of the system, the AFM tip works as a sensor for imaging and an end effector for manipulation. Since interaction force is a key factor for Kalman filter to detect the faulty display, here instead of using traditional AFM tips, an active probe is used to get a high sensitive force feedback [13]. The bottom middle is the augmented reality interface. The augmented reality interface provides enhanced media for the operator to view the real-time movie-like AFM image and feel the real-time force feedback during manipulation. The top middle is the real-time control module, which includes an active probe controller, a Kalman filter and a local scan controller. These are the new added parts comparing with the original augmented reality system, through which the reality of the visual feedback is greatly improved. In the conventional augmented reality system, the movie-like visual display is calculated based on the real time interaction force and behavior models. No schemes check the validity of the visual display, thus its reliability can not be guaranteed due to the uncertainties in nano-environment. To solve this problem, RFDC method is developed and implemented into the system. The flow chart of the RFDC enhanced system is shown in Fig. 2. Since random drift aroused from an uncontrolled manipulation environment generates a position error between the manipulation coordinate and the true environment, an initial random drift compensation needs to be performed first before manipulation starts [14]. After manipulation begins, by actively controlling the rigidity of the active probe's cantilever, a high sensitive interaction force is obtained through the active probe controller, based on which the manipulation process is monitored in real time by the developed Kalman filter. The mismatch between the visual display and the true environment can be detected through the real-time updated Kalman filter residual. Once the error is detected, local scan is performed to obtain the true manipulation results. Finally, the fault display is real-time corrected by the true manipulation results.

From above introduction we can see, in this new designed system, the visual feedback is updated not only relying on the behavior model, but also based on the real-time data from RFDC process. In this way, the visual display keeps consistent with the true environment changes, which in turn facilitates the AFM based nanomanipulation.

III. REAL-TIME FAULT DETECTION AND CORRECTION

As introduced in section I, the movie-like visual feedback in visual reality environment is not the real changes of the nano-environment, but calculated from the behavior models. Since any model may have difference with the true environment changes, the modeling errors will result in a fault display and lead to a failed manipulation. To solve this problem, a Kalman filter and local scan scheme are developed in this section to detect and correct the fault display in real-time. Here Kalman filter is not only used to detect the fault display, but also used to generate the optimal scan patterns for minimizing the local scan time.

A. Kalman filter based Faulty Display Detection

The object's dynamic model is necessary to detect the error between the visual feedback and the the true environment changes by using Kalman filtering techniques. To make our point more clear, an example of manipulating nano-particle will be used to explain this method. This method can be expanded to other tapes' objects by adopting corresponding dynamic models. To simplify the analysis, the motion of tip and objects is decomposed into two directions X and Y. The

dynamic model of the nano-particle in X direction during manipulation can be expressed as:

$$\ddot{x} + k\dot{x} = \lambda F_x \tag{1}$$

Here x is the relative displacement of the particle to the pushing start point in X direction, F_x is the interaction force between the particle and the AFM tip measured from the active probe controller, k is the damping coefficient of the tip-object dynamic system, λ is the proportional gain for adjusting the sensed interaction force. k and λ can be determined through experiments. The similar equation can be written for Y direction. The state space representation of the nano-particle in X direction is:

$$\begin{cases} \dot{x} &= v_x \\ \dot{v}_x &= \lambda F_x - k v_x \end{cases} \tag{2}$$

Here x, v_x are the displacement and velocity of the particle in X direction respectively.

The corresponding discrete-time equations in X and Y direction with a sampling period T can be retrieved from equation (2) as:

$$\begin{cases} X_{k+1} = AX_k + BU_k \\ Z_k = CX_k \end{cases} \tag{3}$$

Where $X_k = [x_k, y_k, \dot{x}_k, \dot{y}_k]^T$, $U_k = [0, 0, f_k^x, f_k^y]^T$, here f_k^x and f_k^y is the interaction force in X and Y direction respectively. Z_k is the states measurement from the visual display, the observation matrixes C is a 4-by-4 unit matrix, state transition matrix A and control input matrix B are given as:

$$A = \begin{bmatrix} 1 & 0 & \frac{1}{k}(1-e^{-kT}) & 0 \\ 0 & 1 & 0 & \frac{1}{k}(1-e^{-kT}) \\ 0 & 0 & e^{-kT} & 0 \\ 0 & 0 & 0 & e^{-kT} \end{bmatrix}$$

$$B = \begin{bmatrix} 0 & 0 & \frac{\lambda}{k}(T - \frac{1}{k} + \frac{1}{k}e^{-kT}) & 0 \\ 0 & 0 & 0 & \frac{\lambda}{k}(T - \frac{1}{k} + \frac{1}{k}e^{-kT}) \\ 0 & 0 & \frac{\lambda}{k}(1-e^{-kT}) & 0 \\ 0 & 0 & 0 & \frac{\lambda}{k}(1-e^{-kT})) \end{bmatrix}$$

With the dynamic model of the object, it is now possible to test if the visual display agrees with the real time changes in the nano environment or not. This is done by monitoring the residual of the Kalman filter. An estimate $X_{k/k-1}$ and an associated covariance matrix $P_{k/k}$ are real-time calculated during manipulation. In the ideal case, without error the residual e_k from the Kalman filter should be Gaussian and white. e_k is defined as:

$$e_k = Z_k - CX_{k/k-1} \tag{4}$$

When the visual display does not agree with the estimation, the innovation e_k will not be Gaussian nor white. The value of $e_k^T e_k$ will has an abrupt increase. $e_k^T e_k$ can be directly used to judge whether there is a display error by setting a threshold on it. But this way is less robust and false alarm signals are frequently triggered. To improve the robustness of the fault detection, Mahalanobis distance of the innovation e_k is calculated and used as a measurement to determine whether there is a fault display [15]. The Mahalanobis distance is defined as:

$$M_t = e^T R_e^{-1} e \tag{5}$$

Where R_e is the associated covariance of e_k and defined as:

$$R_e = E[(Z_k - CX_{k/k-1})(Z_k - CX_{k/k-1})^T] \tag{6}$$

Substituting $Y_k = CX_k + V_k$ into (6) (here V_k is the measurement noise with the covariance R and independent of X_k). Equation (6) can be rewritten as:

$$R_e = P_{k/k} + R \tag{7}$$

By substituting equation (7) into equation (5), the Mahalanobis distance M_t can be real-time obtained during manipulation. A threshold on M_t is set to give an alarm signal when a fault happens. Once the visual display loses match with the real environment changes, M_t will have an abrupt increase and overshoot the threshold. An alarm signal will be triggered for reporting the display error to the system.

B. Local Scan based On-Line Faulty Display Correction

The traditional way to correct the faulty display has to get a new image scan, then update the visual display with the new AFM image to continue manipulation successfully. Although this way can correct the position error, it takes time to get a new AFM image and manipulation has to be interrupted, which is time-consuming and makes AFM based manipulation lack efficiency.

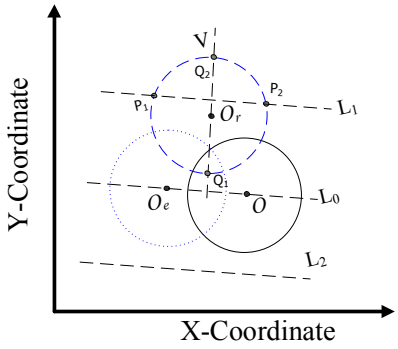

Fig. 3. Local scan pattern for correcting the fault display.

Since only local surface feature is changed during manipulation, after the fault display is detected, a fully image scan is not necessary. The real manipulation result can be obtained by scanning several lines. The faulty display can be corrected by locally updating the visual display with the local scan result. As mentioned above, with the estimation of the Kalman filter, the scan pattern can be optimized to minimize the local scan time. The optimized scan pattern should first scan the area with the highest probability that the object can be found. Since Kalman filter can provide an optimal estimation of the true position, the scan pattern is designed as shown in Fig.

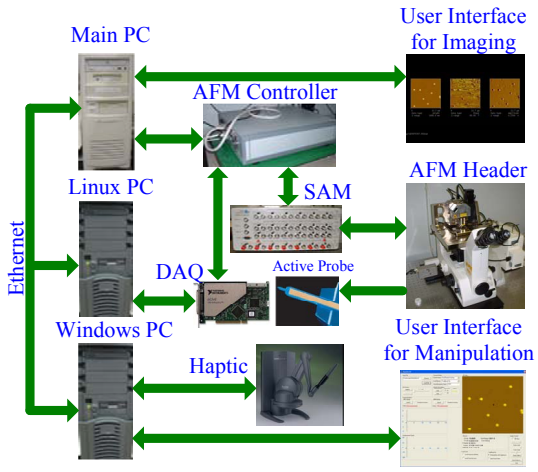

Fig. 4. The configuration of the augmented reality system enhanced by on-line sensing and display.

3. The solid circle O represents the particle position in the visual display interface. The dotted circle O_e represents the estimation position from the Kalman filter. In an ideal case, the particle's real position should agree with the estimated position from Kalman filter. Due to the environment noise or the dynamic modeling errors, the real position of the particle may not be at point O_e, but at point O_r. The scan pattern will first go along line L_0, which passes through the displayed center O and the estimating center O_e. If the particle was not found, then the scanning line moves up and down along the direction perpendicular to line L_0 alternatively by a distance of 3/2*R* until the particle is found, where *R* is the radius of the particle. Once the particle is found, the scanning line forms two intersection points with the boundary of the particle, P_1 and P_2. Another line V, which goes through the midpoint between P_1 and P_2 and is perpendicular to the previous scanning line, is scanned to get the actual center O_r of the particle. The last scan line has two intersection points with the boundary of the particle, Q_1 and Q_2. The final actual center of the nano-particle O_r, located at the midpoint between Q_1 and Q_2. By first scanning the estimated position of the Kalman filter, the object can often be found by the first scan line, which shortens the local scan time, as well as smooths the visual feedback and makes local scan transparent to the operator.

IV. IMPLEMENTATION AND EXPERIMENTAL RESULTS

The experiments were performed in an ambient condition. The configuration of the experimental system is shown as in Fig. 4. It mainly consists of a NanoScope IV Atomic Force Microscope (Vecco Inc., Santa Barbara, CA) with a scanner with a maximum XY scan range of 90μm×90μm and a Z range of 5μm. Some peripheral devices including a haptic device (Phantom, Sensable Company, Woburn, MA), a Multifunction Data Acquisition (DAQ) cards NI PCI-6036E (National Instruments) and three computers. To speed up local scan, the AFM controller has been modified here. The drive signals of the AFM scanner for local scan need not to be transferred by software, but directly outputted to the AFM controller through DAQ card by the Linux PC.

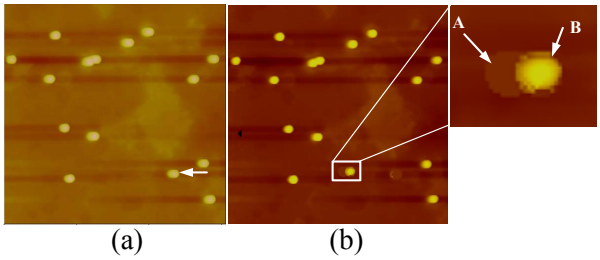

Fig. 5. Manipulating latex particles (diameter 350nm) on polycarbonate surface with an operation range of 12μm. (a) Pushing a particle along the arrow direction; (b) Manipulation result in the visual display. The right picture is the zoom in image of the rectangle area in (b). The indent A represents the false display position. B represents the true position which is online obtained by local scan.

In this experiment, nano-particles are manipulated to validate the effectiveness and efficiency of the RFDC method. The parameter k and λ in equation (2) are obtained from experiments with value 2.2 and 1 respectively. As shown in Fig. 5(a), a latex particle with diameter around 350nm was pushed along the arrow direction. Fig. 6(a) shows the real-time interaction force between the AFM tip and the particle during manipulation. Based on the interaction force, the behavior state of the particle estimated from the Kalman filter is shown as the dashed line in Fig. 6(b). The solid line in Fig. 6(b) is the measured behavior state from the visual display interface. The corresponding residual from the Kalman filter is shown in Fig. 6(c). Before $t = 5.8s$, the behavior state in the visual display agrees with the Kalman filter estimation. The residual value keeps near zero and is less than the threshold. After

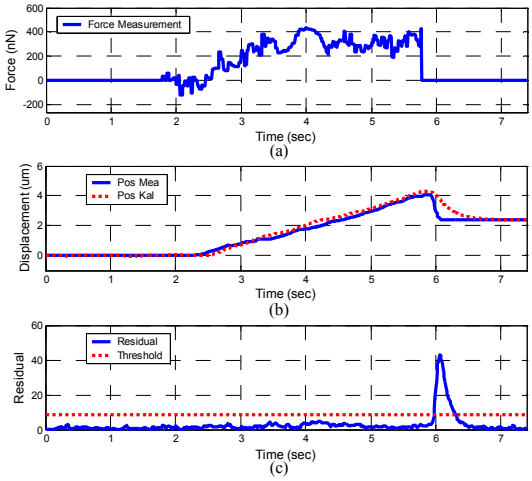

Fig. 6. Kalman filter based error detection. (a) The real-time interaction force between the particle and the AFM tip during manipulation; (b) Position displayed in the visual feedback (the solid line) and position estimated from Kalman filter (the dashed line); (c) The Mahalanobis distance based residual.

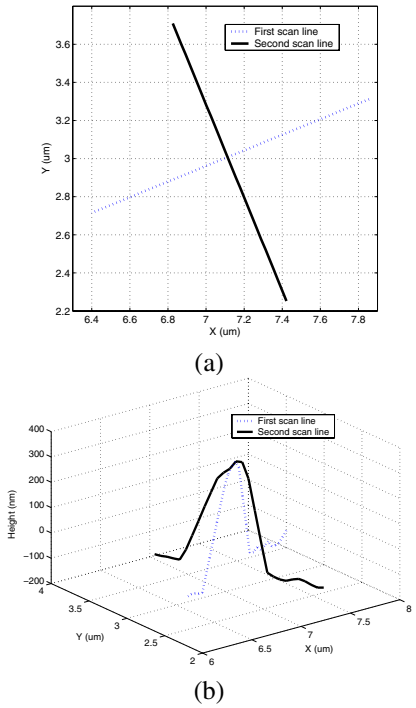

Fig. 7. Local scan pattern and result. (a) The local scan pattern for nano-particles; (b) The topography information along the searching lines.

$t = 5.8s$, the residual has an abrupt increase and overshoots the threshold, which means the visual display does not agree with the true environment changes any longer, and a fault display is detected. This phenomenon agrees with the change of the interaction force as shown in Fig. 6(a), at $t = 5.8s$, there is a sudden drop of the interaction force, which means the tip may slip away from the particle. As a result, the estimated displacement from Kalman filter does not agree with the visual display any more after $t = 5.8s$. Therefore, the residual sharply increased and an alarm signal is triggered for reporting this error to the system.

After the alarm signal was triggered, an optimized scan pattern was generated based on the estimation from the Kalman filter as shown in Fig. 7(a). The topography information along the scanning lines is shown in Fig. 7(b). From the topography information, the actual position of the nano-particle can be identified and updated to the display. As shown in Fig. 5(b), the indent area A represents the particle location in the visual display. Area B shows the real particle position detected from the local scan. The difference between position A and position B demonstrates that the faulty display caused by the modeling error or other uncertainties is effectively detected by the Klaman filter and also corrected through the local scan method.

Fig. 5 demonstrates an often happened case in AFM based manipulation that the AFM tip is easy to slip over or slip away from the object. This situation is difficult to be predicted with behavior models, which often results in a fault visual feedback and leads to a failed manipulation. As shown in Fig.

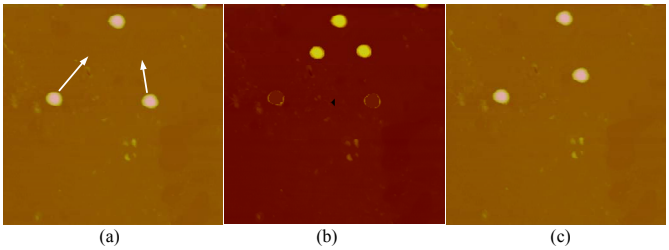

Fig. 8. Manipulating latex particles (diameter 350nm) on polycarbonate surface without the assistance of RFDC method. The operation range is $7\mu m \times 7\mu m$. (a) Manipulating two particles along the arrow directions. (b) The image of manipulation result displayed in the real-time visual feedback interface; (c) a new scanned AFM image after final manipulation.

8, two particles were manipulated along the arrow direction using the original augmented system without RFDC method. Fig. 8(b) is the real-time display interface which illustrates that the particles have been manipulated to their destination positions. Since the visual display was not validated by RFDC method, its reliability can not be guaranteed. As shown in Fig. 8(c), the true manipulation result was obtained through a new image scan. Obviously, the display in the visual feedback interface does not match the true manipulation result due to the inaccurate models in the manipulation process. Without RFDC method, a new image scan is repeatedly needed to verify the manipulation result and correct the faulty display for building some complicated nano-structures, which is time-consuming and low efficient. After incorporating RFDC method, the AFM based nanomanipulation is greatly facilitated. Not only the manipulation process can be real-time monitored, but also the mismatch between the visual display and true environment can be corrected on-line without interrupting manipulation. Operator can immediately know the result after each step of manipulation. Fig. 9 shows a special pattern built by manipulating nano-particles under the assistance of RFDC. The real-time AFM image is displayed in the augmented reality interface as shown in Fig. 9(b). A new scanned image after manipulation is shown in Fig. 9(c). These pictures show that the final result matches the real-time visual display well. Under the assistance of RFDC, the pattern were formed continuously in a couple of minutes. Without the assistance of RFDC, it often took several tens of minutes to form a pattern as shown in Fig. 9 due to repetitively scanning new AFM images. From the experimental study, it can be seen that assembly of nano-structures using RFDC enhanced augmented reality system become very straightforward and high efficient.

V. CONCLUSIONS

It is well known that the main difficulty of nanomanipulation using AFM is the lack of real-time visual feedback. Due to this reason, the manipulation task can not be performed as in the macro world. As a result, a new AFM image scan is repetitively needed to finish the manipulation task successfully, which makes the AFM based nanomanipulation time-consuming and low efficient due to the slow speed of the

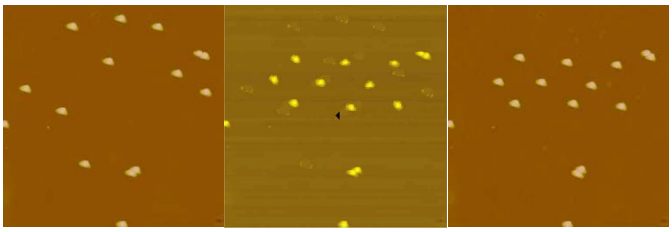

(a) (b) (c)

Fig. 9. Manipulating nano-particles with diameter 350nm on polycarbonate surface. The operation range is $15\mu m \times 15\mu m$. (a) Image of latex particles on a polycarbonate surface before manipulation; (b) The image of manipulation result displayed in the real-time visual feedback interface; (c) a new scanned AFM image after final manipulation.

AFM image scan. This paper introduced a RFDC method to solve this problem. By real-time monitoring the manipulation process, the random drift and the modeling errors are detected and corrected on-line. The manipulation is always carried out with the visual feedback of the true environment changes, through which the efficiency and effectiveness of the AFM based nanomanipulation are greatly improved.

The developed method also provides a facilitated 'bottom-up' technology to built irregular and nonsymmetric nanostructures. Since building nonsymmetric nanostructures using 'top-down' method has been hindered due to the limitations that the smallest feature that can be made must be larger than half of the wavelength of the light used in the lithography. The developed method has a lot of potential applications in manufacturing new revolutionary products under nanoscale, which will bring breakthroughs to the modern society in the future.

VI. ACKNOWLEDGMENTS

This research work is partially supported under NSF Grants IIS-9796300, IIS-9796287, EIA-9911077 and DMI-0500372. The authors would like to thank Dr. Chanmin Su of Veeco Instrument Inc. for his technical advice and help during the process of this research.

REFERENCES

[1] G. Binning, C. F. Quate, and C. Gerber. "Atomic force microscope," *Physical Review Letters*, vol. 56, no. 9, pp. 930-933, 1986.

[2] D. M. Schaefer, R. Reifenberger, A. Patil, and R. P. Andres. "Fabrication of two-dimensional arrays of nanometer-size clusters with the atomic force microscope." *Applied Physics Letters*, Vol. 66, pp. 1012-1014, February 1995.

[3] D. Wang, L. Tsau, et al. "Nanofabrication of thin chromium film deposited on Si(100) surfaces by tip induced anodization in atomic force microscopy." *Applied Physics Letters* vol. 67(9), pp. 1295-1297.

[4] Y. Kim and C. M. Lieber. "Machining oxide thin films with an atomic force microscope: pattern and objective formation on the nanometer scale," *Science,* vol. 257, no. 5068, pp. 375-377, 1992.

[5] D. M. Schaefer, R. Reifenberger, A. Patil, and R. P. Andres. "Fabrication of two-dimensional arrays of nanometer-size clusters with the atomic force microscope," *Applied Physics Letters,* vol. 66, pp. 1012-1014, February 1995.

[6] T. Junno, K. Deppert, L. Montelius and L. Samuelson. "Controlled manipulation of nanoparticles with an atomic force microscope," *Applied Physics Letters,* vol. 66, pp. 3627-3629. 1995

[7] R. Resch, C. Baur, A. Bugacov, B. E. Koel, A. Madhukar, A. A. G. Requicha, and P. Will. "Building and manipulating three-dimensional and linked two-dimensional structures of nanoparticles using scanning force microscopy," *Langmuir,* vol. 14, no. 23, pp. 6613-6616, November 1998.

[8] L. T. Hansen, A. Kuhle, A. H. Sorensen, J. Bohr, and P. E. Lindelof. "A technique for positioning nanoparticles using an atomic force microscope," *Nanotechnology,* vol. 9, pp. 337-342, 1998.

[9] M. Sitti and H. Hashimoto, "Tele-nanorobotics using atomic force microscope," in *Proc. IEEE Int. Intelligent Robots Systems Conf.,* Victoria, BC, Canada, pp. 1739-1746, 1998.

[10] M. Guthold, M. R. Falvo, W. G. Matthews, S. Washburn, S. Paulson, and D. A. Erie, "Controlled manipulation of molecular samples with the nanomanipulator," *IEEE/ASME Trans on Mechatronics,* vol. 5, no. 2, pp. 189-198, Jun. 2000.

[11] G. Li, N. Xi, M. Yu, and W. Feng, "Development of augmented reality system for AFM-based nanomanipulation," *IEEE/ASME Transactions on Mechatronics,* vol. 9, pp. 358-365, 2004.

[12] G. Li, N. Xi, H. Chen, S. Ali, and M. Yu, "Assembly of nanostructure using AFM based nanomanipulation system," *In 2004 IEEE International Conference on Robotics and Automation*, vol. 1, pp. 428-433.

[13] J. Zhang, N. Xi, G. Li, H. Y. Chan, and U. C. Wejinya, "Adaptable End Effector for Atomic Force Microscopy Based Nanomanipulation," *IEEE Transactions on Nanotechnology,* vol. 5, pp. 628-642, 2006.

[14] Lianqing Liu, Jiangbo Zhang, Guangyong Li, Ning Xi. "On-line sensing and display in Atomic Force Microscope based nanorobotic manipulati On-line sensing and display in Atomic Force Microscope based nanorobotic manipulation." *In 2007 IEEE/ASME International Conference on Advanced Intelliget Mechatronics,* vol. 1, pp. 1-6.

[15] P. M. Frank, "Fault diagnosis in dynamic systems using analytical and knowledge-based redundancy : A survey and some new results." *Automatica* vol. 26, pp. 459-474, 1990.